

Electronic Supplementary Information

Single-molecule force spectroscopy to decipher the early signalling step in membrane-bound penicillin receptors embedded in a lipid bilayer

Andrea Mescola^a, Marjorie Dauvin^b, Ana Amoroso^b, Anne-Sophie Duwez^a and Bernard Joris^b

^aMolecular Systems, Department of chemistry, University of Liège, 4000 Liège, Belgium.

^bBacterial physiology and genetics - Centre d'Ingénierie des Protéines- Integrative Biological Sciences,
Department of Life Sciences, Liège University. Sart-Tilman B6a, 4000 Liège, Belgium.

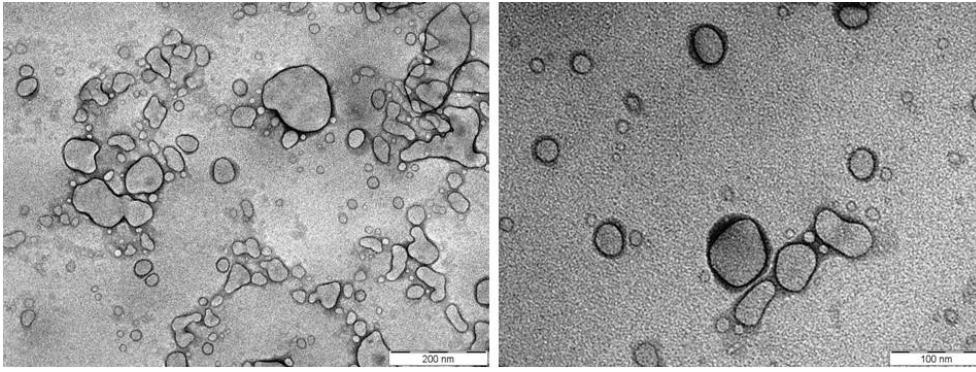
Name	Nucleotide sequence	Comments
pET28aBlaRTwinSTII_RV	5'-CAA-GCG-CTT-GCG-GCC-GCT- CGG-GAA-ACG-GAG-GGA-TAA-ATC-CC-3'	Amplification of <i>blaR1</i> - E ²¹³ A and cloning in pET28 Twin-STII
BlaR_BamHI_NcoI_5'	5'-TAT-TGC-GGA-TCC-CAT-GGG-CAG- CAG-TTC-TTT-CTT-TAT-TCC-C-3'	
TwinStrepT_UP	5'-GAC-AAG-CTT-GCG-GCC-GCA-AGC- GCT-TGG-AGC-CAC-CCG-CAG-TTC-GAG- AAA-GGT-GGA-GGT-TCC-GGA-GGT-GGA- TCG-GGA-GGT-GGA-TCG-TG-3'	<i>tStrep-tag</i>
TwinStrepT_RP	5'-TGG-TGG-TGG-TGC-TCG-AGT-TAT-TAT- TTT-TCG-AAC-TGC-GGG-TGG-CTC-CAC- GAT-CCA-CCT-CCC-GAT-CCA-CCT-CCG- GAA-CCT-CCA-CCT-T-3'	
Poly-gly	5'-GCG-GCC-GCG-GGC-GGC-GGT-GGT- GGG-GGA-GGT-GGT-GGT-GGA-GGT-GGA- GGA-GGC-GGA-GGT-GGA-GGA-GGC-GGT- GGC-GGT-GGC-GGC-GGA-GGT-GGC-GGC- GGA-GGA-GGG-GGA-GGC-GGA-GGC-GGC- GGG-GGC-GGC-GGA-GCG-GCC-GC-3'	<i>poly-Gly</i> ₄₀ linker
Polyglyinf-FW	5'-GTT-TCC-CGA-GCG-GCC-GCG-GGC- GGC-GGT-GGT-GGG-G-3'	Amplification and cloning of <i>poly-Gly</i> ₄₀ linker in pET28
Polyglyinf-RV	5'-CAA-GCG-CTT-GCG-GCC-GCT-CCG-CCG- CCC-CCG-CC-3'	
blaRE213A-pHCMC04-Fw	5'-AAT-GGT-CCA-AAC-TAG-TGA-TAT-CAT- GAG-CAG-TTC-TTT-CTT-TAT-TCC-C-3'	Amplification of <i>blaR1</i> and cloning in pHCMC04
blaRE213A-pHCMC04-Rev	5'-GAA-GGA-ATG-AGG-ATC-CTT-ACT-TTT- CGA-ACT-GCG-GGT-GG-3'	
blaRpolygly-RP	5'-CAC-CGC-CGC-CCG-CGG-CCG-CTC- GGG-AAA-CGG-AGG-GAT-AAA-TCC-C-3'	Fusion of <i>poly-Gly</i> ₄₀ to <i>blaR1</i>

Supplementary Table 1. Oligonucleotides used in this study. After amplification and purification plasmid constructions were verified by DNA sequencing (GIGA-DNA sequencing platform, University of Liège).

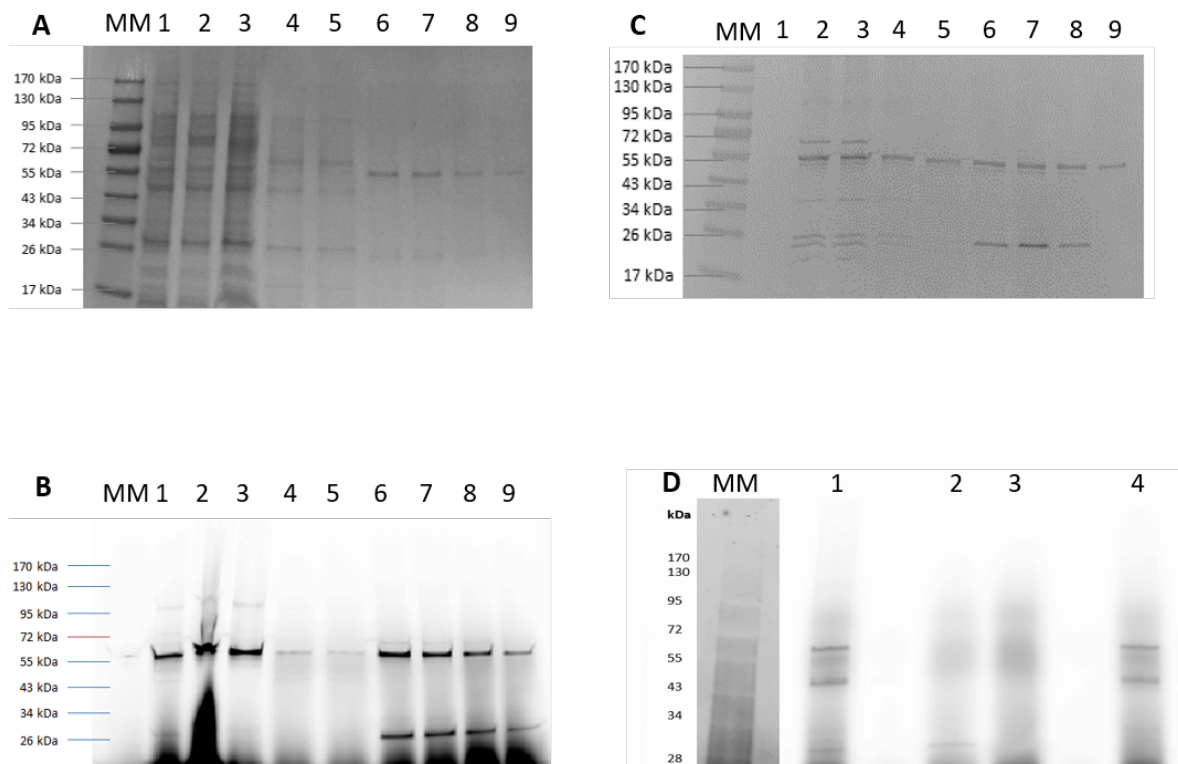
Strain or plasmid	Description and relevant characteristic	Source
pBPG222	pET28a production plasmid derivative carrying DNA sequence encoding tStrep-tag	This study
pDML1256	Plasmid carrying <i>blaR1 E²¹³A</i> mutant	1
pDML995	Plasmid carrying wild type <i>blaR1</i>	2
pJet1.2/Blunt	Cloning vector	ThermoFisher Scientific®
pJet-BlaR1 E ²¹³ A	pJet1.2/Blunt derivative carrying <i>blaR1 E²¹³A</i>	This study
pJet-polyGly	pJet1.2 Blunt End derivative carrying DNA sequence encoding poly-Gly ₄₀ linker	This study
pBPG223	pBPG222 derivative carrying <i>blaR1 E²¹³A</i>	This study
pBPG224	pBPG222 derivative carrying <i>blaR1-E²¹³A-(poly-Gly)₄₀-tStrep-tag</i>	This study
pHCMC04	<i>B. subtilis-E. coli</i> shuttle vector harboring <i>xylR</i> and P _{xylA} promoter	<i>Bacillus</i> Genetic Stock Centre ³
pBPG225	Derivative of pHCMC04 carrying the divergeon <i>gfpmut3</i> and <i>blaI</i> and under the control of P _{bla} , and <i>blaR1</i> under control of P _{xylA} (for details see Figure S1.1).	M. Dauvin, unpublished data
pBPG227	Derivative of ECE189P carrying the divergeon P _{bla} <i>gfpmut3-blaI</i>	This study
pBPG230	Derivative of pBPG225 carrying <i>blaR1-poly-Gly₄₀-tStrep-tag</i>	This study
<i>Escherichia coli</i> BL21 DE3	Host cell for heterologous expression of Bl- <i>blaR1</i> ; <i>fhuA2 [lon] ompT gal (λ DE3) [dcm] ΔhsdSλ DE3 = λ sBamHI ΔEcoRI-B int::(lacI::PlacUV5::T7 gene1) i21 Δnin5</i>	New England BioLabs®Inc.
<i>Bacillus subtilis</i> 168	Host cell for induction assays with pBPG225 and pBPG230	<i>Bacillus</i> Genetic Stock Centre ³

Supplementary Table 2. Plasmids and bacterial strains used in this study.

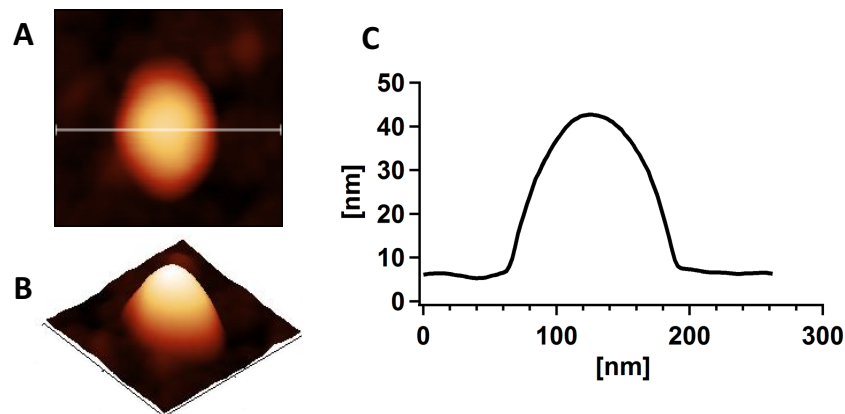
structure are indicated as follows: arrows and rectangles represent β -sheets and α -helices, respectively. The lower numbering is that of Bl-BlaR1 (UniProt:Blar_BacIi) and the upper is the reverse numbering of R-BlaR1 from its C-terminal end. TM: transmembrane segment; L1-3: are loops between TMs; * = indicates E²¹³A mutation in the conserved motif H-E-X-X-H; G₄₀: poly-Gly₄₀.



Supplementary Figure 2. TEM analysis of generated lipid vesicles. The scale bars are 200 nm and 100 nm for (A) magnification $8 \cdot 10^6 \times$ and (B) magnification $15 \cdot 10^6 \times$, respectively.



Supplementary Figure 3. Analysis of R-BlaR1 production, extraction, purification and insertion in LUVs. (A): SDS-PAGE revealed by Coomassie blue staining. 1: membrane fraction; 2: membrane fraction solubilized by n-dodecyl β -D-maltopyranoside detergent (2%, DDM); 3: loading sample; 4-5: wash fractions; 6-9: eluted fractions. (B): SDS-PAGE revealed by penicillin-binding assay: 1: membrane fraction; 2: membrane fraction solubilized by DDM; 3: loading sample; 4-5: wash fractions; 6 to 9, eluted fractions. (C): Western blotting analysis (polyclonal rabbit antibody directed against Bl-BlaR^S). 1: non-induced whole cellular extract; 2: induced membrane fraction solubilized by DDM; 3: loading sample; 4-5: column wash fractions; 6-9: eluted fractions. (D): R-BlaR1 inserted in LUVs analyzed by SDS-PAGE revealed by penicillin-binding assay. 1: concentrated purified R-BlaR1 fraction before its insertion in LUVs; 2-3, wash fractions after R-BlaR1 insertion in LUVs; 4: R-BlaR1 included in LUVs solubilized by SDS. MM: molecular mass marker.



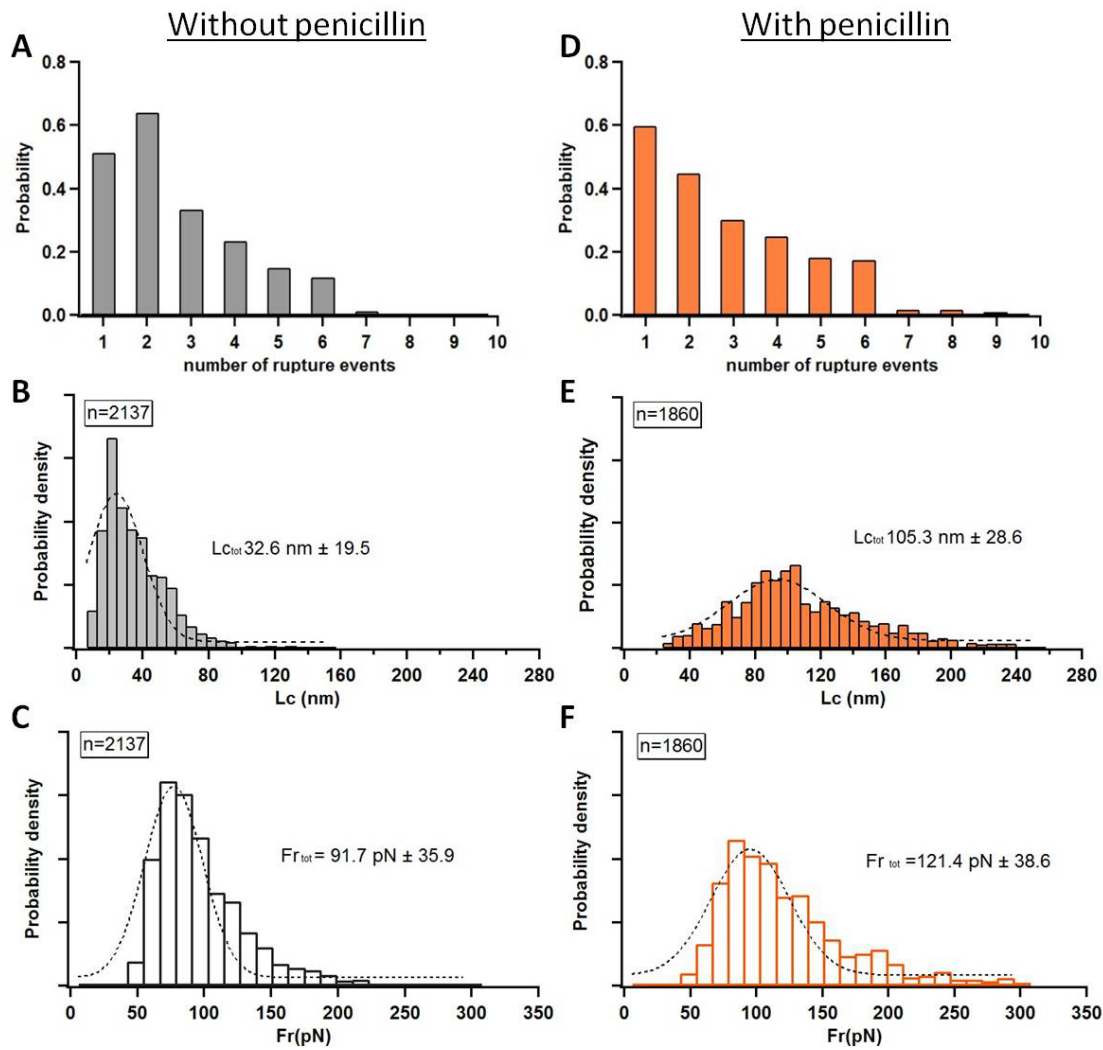
Supplementary Figure 4. Orientation of R-BlaR1 in Supported Lipid Bilayers (SLBs). AFM topographic reconstruction of R-BlaR1 within SBLs on gold surface, after the introduction of gold nanoparticles coupled to streptavidin. Planar and 3D AFM images (A and B). Profile extracted from the planar reconstruction (C). The measured dimensions are highly dependent on the geometry of the tip⁴⁻⁶, therefore, the measured lateral sizes are usually larger than the true dimensions. Following a theoretical approach⁷, it is possible to establish that the width values recorded are consistent with the real size of the object detected.

The original diameter of the Au nanoparticles is around 40 nm. To compare the apparent width given by the AFM images with the original dimension, we used following equation:

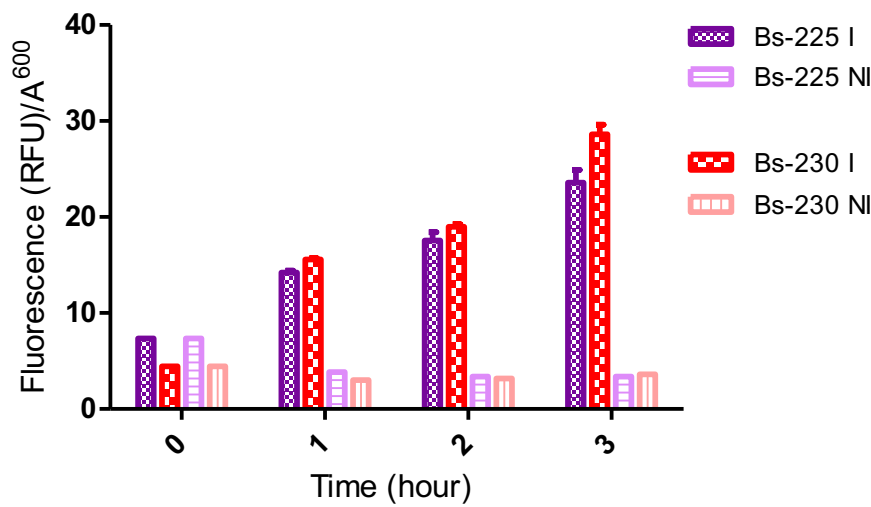
$$d = 4\sqrt{R * r}$$

where d is the apparent width of a spherical feature of radius r scanned by a tip with the radius R . Using the apparent width measured (85 nm) and tip curvature radius, we found a radius of the scanned object around 20 nm that is consistent with the Au nanoparticle dimension.

Thus, we can conclude that the objects revealed by AFM experiments corresponds to the gold nanoparticles, confirming that the sensor domain of R-BlaR1 (BlaR^S) is exposed to the external side of proteoliposomes and accessible to the AFM tip.

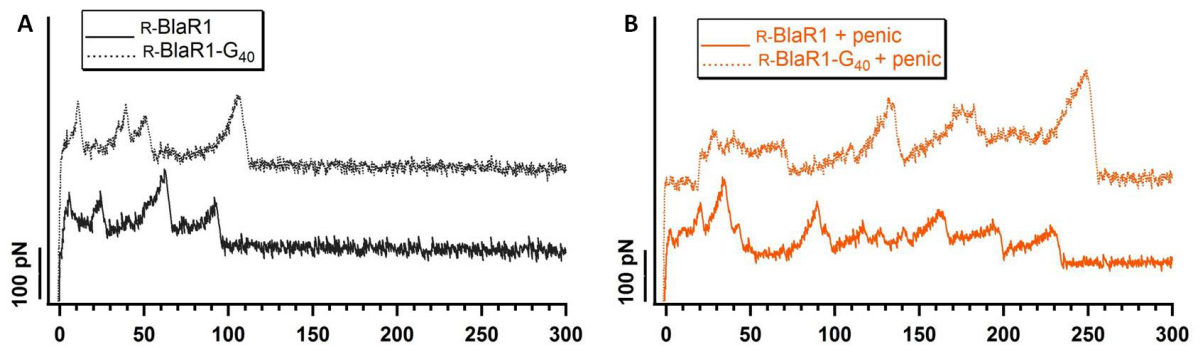


Supplementary Figure 5. Analysis of F-D curves having at least one rupture event, in absence and presence of penicillin. Data analysis including all the F-D curves that have at least one rupture event, in the absence (grey) and in the presence (orange) of penicillin. (A) and (D): probability of number of rupture events in F-D curves. (B) and (E): contour length (L_c) distribution histograms obtained by collecting all the L_c values recorded for each peak detected in all F-D curves. (C) and (F): rupture force (F_r) histograms obtained by collecting all F_r recorded for each peak detected in all F-D curves. B, C, E and F histograms were fitted with single Gaussians (dashed line). L_c and F_r values are shown with their standard deviations. The number F-D curves analyzed are shown in the boxes. For each F-D curve, all the rupture events were fitted with the worm-like-chain (WLC) model to determine the length at maximum extension (contour length, L_c) of the receptor segment that is stretched and unfolded.



Supplementary Figure 6. *R-BlaR1* and *R-BlaR1-G₄₀* induction assays in *B. subtilis* 168.

Induction of GFP-mut3 by *B. subtilis* 168 harboring, respectively, pBPG225 (Bs-225) and pBPG230 (Bs-230) in presence of cephalosporin C. The quantity of GFP-mut3 produced by cell is expressed by Fluorescence/A⁶⁰⁰. The measures are the mean of 3 cultures and error bars represent the 95% confidence interval. Time 0 corresponds to the addition of cephalosporin C (final concentration = 2.5 µg/mL). RFU: Relative Fluorescence Unit; NI: non-induced by cephalosporin C; I: induced by cephalosporin C. pBPG225 and pBPG230 *B. subtilis-E. coli* shuttle vectors allow the expression of, respectively, R-BlaR1 (wild-type receptor) and R-BlaR1-G₄₀ under the control of P_{*xyIA*} promoter. Bs-225 and Bs-230 were assayed for their ability to induce the *gfp-mut3* reporter gene under the control of BlaI repressor. This last one is inactivated by the action of BI-BlaR1 when activated by a β-lactam antibiotic. No significant difference between induced Bs-225 and Bs-230 was observed. This result shows that the addition of Ala₃-Gly₄₀-Ala₃-tStrep-tag (76 residues) at the C-terminal end of BI-BlaR1 does not influence the signal-transduction to the cytoplasm, nor its membrane topology.



Supplementary Figure 7. Comparison of R-BlaR1 and R-BlaR1-G₄₀ F-D curves exhibiting the maximum extension in absence or presence of penicillin. F-D curves exhibiting the maximum extension and recorded from single R-BlaR1 (dashed line) and single C-terminally elongated R-BlaR1 by Ala₃-Gly₄₀ peptide (R-BlaR1-G₄₀, solid line) in absence (A) or in presence of penicillin (B).

Peak class	R-BlaR1		R-BlaR1-G ₄₀		$\Delta\langle L_c \rangle$ (nm)
	$\langle L_c \rangle$ (nm)	σ (nm)	$\langle L_c \rangle$ (nm)	σ (nm)	
I	17.1	5.8	29.2	9.9	12.1
II	39.6	10.2	55.2	11.2	15.6
III	64.5	11.4	79.3	13.9	14.8
IV	78.8	12.9	93.2	15.4	14.4
V	83.2	11.4	98.7	10.5	15.5
VI	88.1	9.1	106.9	8.6	18.8
Mean $\pm \sigma$					15.2 \pm 2.2

Supplementary Table 3. Contour lengths detected upon mechanically unfolding R-BlaR1 and R-BlaR1-G₄₀ from the C-terminal end in absence of penicillin. Most probable contour lengths ($\langle L_c \rangle$) and most probable delta contour length ($\Delta\langle L_c \rangle$, calculated as the distance between two consecutive rupture events of force peak classes). σ : standard deviation.

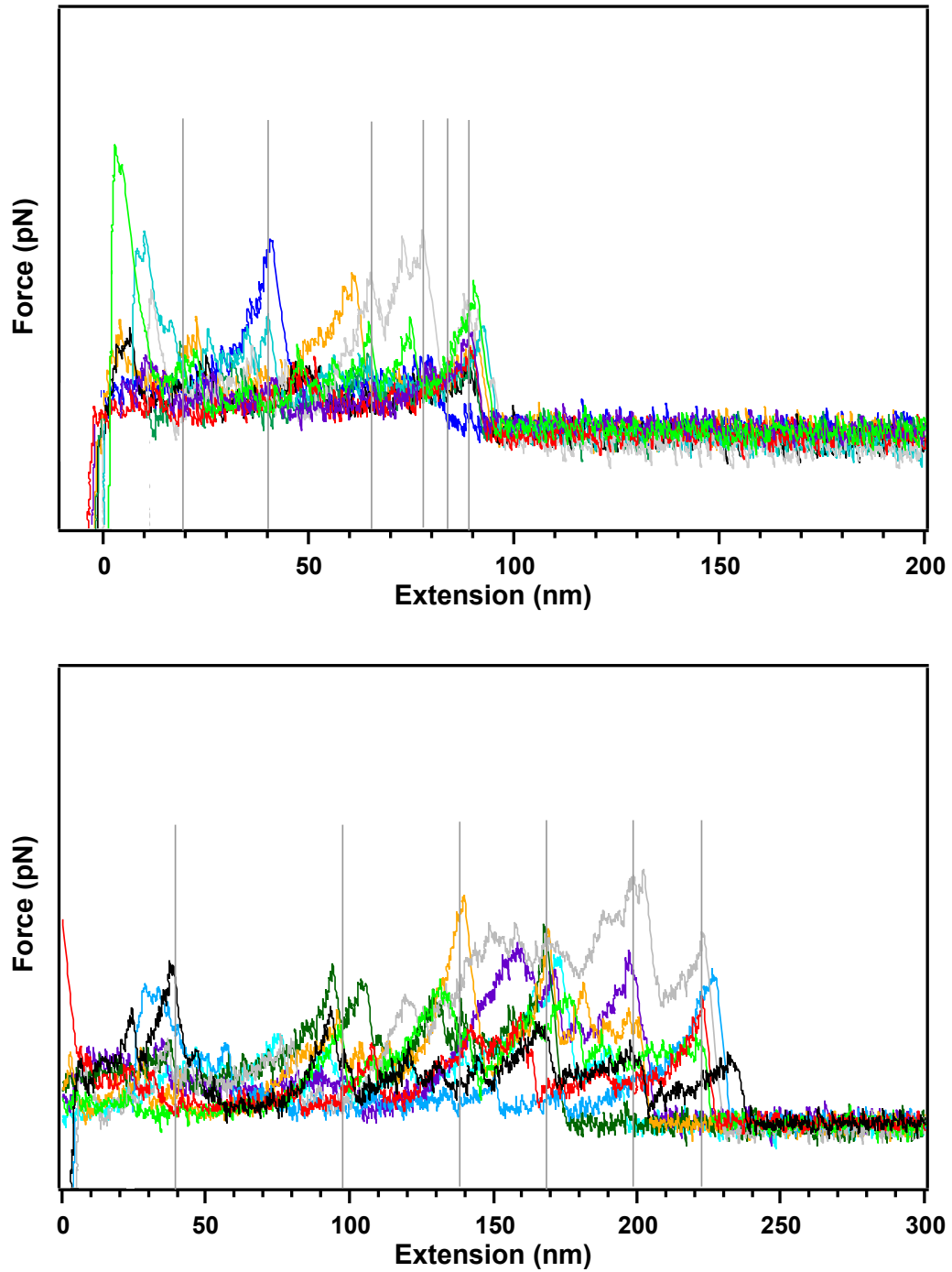
Peak class	R-BlaR1		R-BlaR1-G ₄₀		$\Delta\langle L_c \rangle$ (nm)
	$\langle L_c \rangle$ (nm)	σ (nm)	$\langle L_c \rangle$ (nm)	σ (nm)	
I	40.2	19.2	51.1	22.1	10.9
II	91.5	19.6	105.9	18.8	14.4
III	136.8	18.1	150.9	16.5	14.1
IV	168.4	16.2	183.9	17.1	15.5
V	190.8	11.8	205.1	13.6	14.3
VI	217.5	11.6	232.6	9.8	15.1
Mean \pm σ					14.1 \pm 1.6

Supplementary Table 4. Contour lengths detected upon mechanically unfolding R-BlaR1 and R-BlaR1-G₄₀ from the C-terminal end in presence of penicillin. Most probable contour lengths ($\langle L_c \rangle$) and most probable delta contour length ($\Delta\langle L_c \rangle$, calculated as the distance between two consecutive rupture events of force peak classes). σ : standard deviation.

In absence of penicillin				In presence of penicillin			
Peak classes	L_c (nm)			Peak classes	L_c (nm)		
	Peak analysis	PDF analysis	Single curve		Peak analysis	PDF analysis	Single curve
I	17.1 ± 5.8	18.4 ± 4.9	20.2				
II	39.6 ± 10.2	35.6 ± 4.2	34.2	I	40.2 ± 19.2	38.5 ± 15.9	35.0
		48.7 ± 2.8	45.4				
III	64.5 ± 11.4	63.4 ± 7.0	63.0				
IV	78.8 ± 12.9	75.9 ± 3.9	73.1				
V	83.2 ± 11.4	86.9 ± 6.4					
VI	88.1 ± 9.1			II	91.5 ± 19.6	95.6 ± 12.6	89.7
		98.9 ± 1.6	94.0				
				III	136.8 ± 18.1	121.3 ± 6.9	126.8
				IV	168.4 ± 16.2	153.0 ± 10.9	164.1
				V	190.8 ± 11.8	188.3 ± 12.7	193.3
				VI	217.5 ± 11.6	223.7 ± 2.2	227.6

Supplementary Table 5. Comparison of $\langle L_c \rangle$ values obtained from force peak classes analysis, PDF analysis and single curve analysis in absence and in presence of penicillin.

Grey boxes highlight those segments unfolded in the absence but not in the presence of penicillin.



Supplementary Figure 8. Superimposition of 9 force curves for R-BlaR1 in absence (top panel) or presence of penicillin (bottom panel). The peaks can be classified in 6 classes.

References

- 1 S. Berzigotti, K. Benlafya, J. Sépulchre, A. Amoroso and B. Joris, *PLoS One*, 2012, **7**, 1–10.
- 2 P. Filée, K. Benlafya, M. Delmarcelle, G. Moutzourelis, J.-M. Frère, A. Brans and B. Joris, *Mol. Microbiol.*, 2002, **44**, 685–694.
3. Zeigler, D. R. Bacillus Genetic Stock Center, Columbus, OH.
<http://www.bgsc.org/index.php>. at <<http://www.bgsc.org/index.php>>
- 4 C. Bustamante and D. Keller, *Phys. Today*, 1995, **48**, 32–38.
- 5 Y. Gan, *Surf. Sci. Rep.*, 2009, **64**, 99–121.
- 6 L. Martnez, M. Tello, M. Daz, E. Romn, R. Garcia and Y. Huttel, *Rev. Sci. Instrum.*, 2011, **82**, 1–7.
- 7 P. C. Braga and D. Ricci, *Atomic Force Microscopy in Biomedical Research*, Humana Press, Totowa, NJ, 2011.